Eur. Phys. J. Appl. Phys. **31**, 11–16 (2005)
DOI: 10.1051/epjap:2005036

THE EUROPEAN PHYSICAL JOURNAL APPLIED PHYSICS

Photocurrent simulation in an n-p-n-p silicon multilayer solar cell

A. Bouzidi[a], A.S. Bouazzi, and B. Rezig

Laboratory of Photovoltaic and Semiconductor Materials (LPMS), ENIT, PO Box 37 Tunis, 1012 Tunis-Belvedere, Tunisia

Received: 5 November 2004 / Received in final form: 17 January 2005 / Accepted: 11 February 2005
Published online: 27 April 2005 –

Abstract. In this work, we simulate and optimize the photocurrent densities in a model of an *n-p-n-p* type thin film multilayer silicon solar cell for space applications. The incident light penetrates the cell perpendicularly to the junctions. The electrodes tailored inside the structure connect the *n*-layers together and the *p*-layers together. The equations giving the photocurrent density produced in each abscissa of the structure was developed. We used Matlab software to simulate and optimize the different parameters of the model. The results of simulation show that the optimized *n-p-n-p* silicon multilayer solar cell could deliver a photocurrent density of more than 46 mA/cm^2 under Air Mass 0 (AM0) solar spectrum (solar constant of 1.36 KW/cm^2) and that the photocurrent density produced by the *n-p-n-p* multilayer silicon solar cell is at least 10% higher than the photocurrent density produced by the simple *n-p* junction solar cell. We also show that the most important components of the total photocurrent densities (94%) is due to the minority carrier collection which happens on both side of the three space charge regions tailored inside the cell.

PACS. 72.40.+w Photoconduction and photovoltaic effects – 85.30.De Semiconductor-device characterization, design and modeling

1 Introduction

In the recent years, considerable research effort has been made on the simulation and optimization of high efficiency solar cells, both for terrestrial and space applications. Many theoretical works containing numerical simulation and theoretical prediction models have been devoted to the study of photovoltaic devices to improve their efficiency [1–4].

Merabtine et al. have presented improved optimized silicon and GaAs solar cell performances taking into account the recent techniques of elaboration of a simple *n-p* junction solar cell. The simulation and the optimization of their model have been made using the PCID program solar cell simulator [1].

The recently developed multilayer thin film cell concept has an advantage of improved carrier collection due to a reduced distance from a generated carrier to a junction, this is due to the many depletion regions tailored inside the cell.

Bouazzi et al. have conceived a model of a multilayer silicon solar cell were the emitter is buried. They showed that the short circuit current in the buried emitter solar cell is 10% to 35% higher than the classical cell, depending of surface recombination velocity [2].

Brecl et al. [3] have developed an extended Ebers-Moll model for the examination of the physical parameters of the multilayer cell. They calculate the current-voltage characteristics of floating junction solar cells using the Ebers-Moll model for a certain *p-n-p-n* and *n-p-n-p* tandem, and multilayer silicon solar structures versus the carrier's lifetime, but no effective layers thicknesses optimization has been presented. They showed that the photocurrent density produced by an *n-p-n-p* multilayer solar cell with correspondent layers thicknesses of 0.5 μm, 5.5 μm, 0.4 μm and 30 μm respectively, is equal to 28.19 mA/cm^2 using the global AM1.5 solar spectrum, and 10^3 cm/s surface recombination velocity. A similar model [2] has been studied using minority carriers diffusion equations.

The recombination current was theoretically investigated for a polycrystalline silicon solar cell by Ba et al. [6]. They reported a variation of grain boundary recombination current density with exciting light wavelength for a simple *n-p* junction solar cell.

In our work, we are interested in the simulation and optimization of the photocurrent density in a silicon multilayer solar cell, as it represents an important parameter in the conception of high efficiency solar cells for space applications. This is a first step of a theoretical study to achieve very high efficiency multilayer solar cell for space applications. The next step will be the study of the effect of the layers resistance using the optimal layers thickness to simulate the I–V characteristics of the cell.

The model is composed by four layers of *n-p-n-p* type, including three *n-p* junctions, and it is achieved

[a] e-mail: Abdellatif.bouzidi@isi.rnu.tn

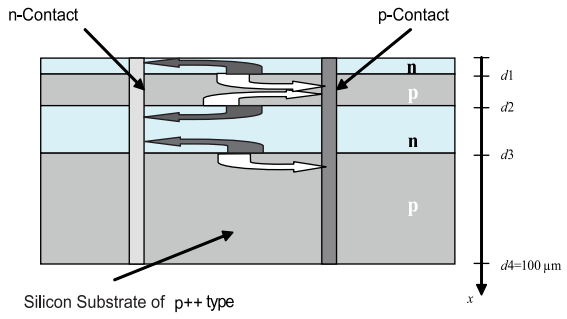

Fig. 1. Cross section of the studied *n*-*p*-*n*-*p* multilayer silicon solar cell, the light enters from the *n*-side.

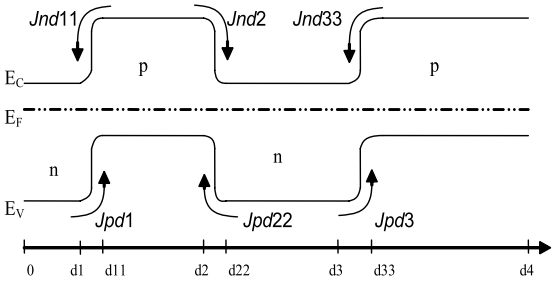

Fig. 2. Energy band structure diagram of the multilayer silicon solar cell. The six arrows show the minority carriers path that produces the photocurrent.

using realistic parameters [5]; the *p*- and *n*-regions contain 10^{17} cm^{-3} of acceptors and donors respectively; in the *p*-layers the electron diffusion coefficient is $D_n = 20$ cm^2/s and the lifetime is $\tau_n = 25$ μs. For the *n*-layers, the holes diffusion coefficient is $D_p = 7$ cm^2/s and the lifetime $\tau_p = 14$ μs. Such quality material can be achieved using several methods. Different fabrication process and cells design have been reported by José Maria Roman [7]; the most used growth methods are molecular organic chemical vapour deposition (MOCVD) and molecular beam epitaxy (MBE) which allowed the fabrication of high quality materials and control over doping profiles of the layers.

In our work, the surface recombination velocity is taken equal to 10^5 cm/s. We used the solar spectrum Air Mass 0 to simulate the photocurrent densities produced in each point of our model, i.e. 1360 W/m^2 incident power, which is the solar power received outside the atmosphere.

A cross section of the studied multilayer silicon solar cell is presented in Figure 1. The abscissas $d1$, $d2$ and $d3$ are respectively the first layer of *n*-type abscissa, the second layer of *p*-type abscissa and the third layer of *n*-type abscissa. The total structure thickness is taken equal to 100 μm, which is widely used in thin film silicon solar cells [8–11], and which assures the mechanical rigidity of the structure. Any electron-hole pair created in each layer of the cell meets the nearest depletion region and is separated, so the hole joins the *p*-contact and electron joins the *n*-contact. The photocurrent density produced by each layer results from the collection of the photogenerated minority carriers; the electrons in the *p*-type regions and the holes in the *n*-type regions.

2 Photocurrent densities calculation

In our model, we suppose that the vertical electrodes are tailored in such a way that they can collect all the photocurrent generated in the cell without any losses. We also suppose that the structure is fully homogeneous and that there is no default in the layers growth, which allowed us to use a one dimensional model to calculate and to simulate the photocurrent density (the short circuit current density) generated.

Figure 2 shows the energy band structure diagram of our model. The region between the abscissa $d1$ and $d11$ represents the first space charge region, the region between $d2$ and $d22$ represents the second space charge region and the region between $d3$ and $d33$ represents the third space charge region. $Jpd1$ represents the photocurrent density that outcomes from the light absorbed in the first layer, $Jnd11$ and $Jnd2$ represents the photocurrent density that results from the absorbed light in the second layer, $Jpd22$ and $Jpd3$ represents the photocurrent density that results from the absorbed light in the third layer. Finally, $Jnd33$ represents the photocurrent density that results from the absorbed light in the four layer of *n*-type.

The classical diffusion equations are:
in the *n*-type region:

$$D_p \frac{\partial^2 P}{\partial x^2} - \frac{P}{\tau_p} + G(x) = 0 \tag{1}$$

and in the *p*-type region:

$$D_n \frac{\partial^2 n}{\partial x^2} - \frac{n}{\tau_n} + G(x) = 0 \tag{2}$$

where p and n are the concentration of the minority carriers, D is the diffusion coefficient, τ is the lifetime and $G(x)$ is the generation function given by:

$$G(x) = \phi(\lambda)\alpha(\lambda)\exp(-\alpha(\lambda)x). \tag{3}$$

The boundary conditions to solve these equations are as follows [2]:

$$qD_p \frac{\partial p}{\partial x}\bigg|_{x=0} = qpS \,\text{and}\, p(d1) = 0. \tag{4}$$

$$n(x) = 0 \,\text{at}\, x = d11 \,\text{and}\, x = d2 \tag{5}$$

$$p(x) = 0 \,\text{at}\, x = d22 \,\text{and}\, x = d3 \tag{6}$$

$$n(x) = 0 \,\text{at}\, x = d33 \tag{7}$$

$$qD_n \frac{\partial n}{\partial x}\bigg|_{x=d4} = qnS'. \tag{8}$$

The photocurrent density is calculated, at the edges of the junctions, form the concentration of the minority carriers as follows:
for the holes in the *n*-type region

$$J_p = qD_p \frac{\partial p}{\partial x} \tag{9}$$

$$p(x) = \frac{\alpha\phi L_p^2}{D_n\left(1-\alpha^2 L_p^2\right)} \left\{ \frac{L_p\left(\frac{S}{D_p}+\alpha\right)\sinh\left(\frac{x-d1}{L_p}\right) - e^{-\alpha d1}\left(\cosh\left(\frac{x}{L_p}\right) + \left(\frac{SL_p}{D_p}\right)\sinh\left(\frac{x}{L_p}\right)\right)}{\cosh\left(\frac{d1}{L_p}\right) + \frac{SL_p}{D_p}\sinh\left(\frac{d1}{L_p}\right)} + e^{-\alpha x} \right\}. \quad (11)$$

$$n(x) = \frac{\alpha\phi L_n}{D_n(1-\alpha^2 L_n^2)} \left\{ e^{-\alpha x} + \frac{e^{-\alpha d33}\left[\cosh\left(\frac{x-d4}{L_n}\right) + \frac{SL_n}{D_n}\sinh\left(\frac{x-d4}{L_n}\right)\right] - \left(\alpha L_n + \frac{SL_n}{D_n}\right)e^{-\alpha d4}\sinh\left(\frac{x-d33}{L_n}\right)}{\frac{SL_n}{D_n}\sinh\left(\frac{d4-d33}{L_n}\right) - \cosh\left(\frac{d4-d33}{L_n}\right)} \right\} \quad (16)$$

$$Jn_{d33} = \frac{q\alpha\phi L_n}{1-\alpha^2 L_n^2} \left\{ \alpha L_n e^{-\alpha d33} - \frac{e^{-\alpha d33}\left[\sinh\left(\frac{d33-d4}{L_n}\right) + \frac{SL_n}{D_n}\cosh\left(\frac{d33-d4}{L_n}\right)\right] - \left(\alpha L_n + \frac{SL_n}{D_n}\right)e^{-\alpha d4}}{\frac{SL_n}{D_n}\sinh\left(\frac{d4-d33}{L_n}\right) - \cosh\left(\frac{d4-d33}{L_n}\right)} \right\}. \quad (17)$$

and for the electrons in the *p*-type regions

$$J_n = -qD_n\frac{\partial n}{\partial x}. \quad (10)$$

We give below the equations that express the minority carrier concentration versus the abscissa x in each layer of the cell. The photocurrent density is calculated using equations (9, 10). For the first layer; x between 0 and $d1$, the concentration of the excess minority carrier (holes) is given by:

See equation (11) above.

The photocurrent density produced at $x = d1$ is given by:

$$Jp_{d1} = \frac{q\alpha\phi L_p}{1-\alpha^2 L_p^2} \left\{ \alpha L_p e^{-\alpha d1} - \frac{\frac{SL_p}{Dn} + \alpha L_p - e^{-\alpha d1}\left(\sinh\left(\frac{d1}{L_p}\right) + \frac{SL_p}{D_p}\cosh\left(\frac{d1}{L_p}\right)\right)}{\frac{SL_n}{Dn}\sinh\left(\frac{d1}{L_n}\right) + \cosh\left(\frac{d1}{L_n}\right)} \right\}. \quad (12)$$

For the second layer; x between $d11$ and $d2$, the concentration of the electrons is:

$$n(x) = \frac{\alpha\phi L_n^2}{D_n\left(1-\alpha^2 L_n^2\right)} \times \left\{ \frac{e^{-\alpha d11}\sinh\left(\frac{x-d2}{L_n}\right) - e^{-\alpha d2}\sinh\left(\frac{x-d11}{L_n}\right)}{\sinh\left(\frac{d2-d11}{L_n}\right)} + e^{-\alpha x} \right\} \quad (13)$$

$$Jn_{d11} = -\frac{q\alpha\phi L_n}{1-\alpha^2 L_n^2} \times \left\{ \alpha L_n e^{-\alpha d11} - \frac{e^{-\alpha d11}\cosh\left(\frac{d11-d2}{L_n}\right) - e^{-\alpha d2}}{\sinh\left(\frac{d2-d11}{L_n}\right)} \right\} \quad (14)$$

$$Jn_{d2} = \frac{q\alpha\phi L_n}{1-\alpha^2 L_n^2} \times \left\{ \alpha L_n e^{-\alpha d2} - \frac{e^{-\alpha d11} - e^{\alpha d2}\cosh\left(\frac{d2-d11}{L_n}\right)}{\sinh\left(\frac{d2-d11}{L_n}\right)} \right\}. \quad (15)$$

For the third layer; x between $d22$ and $d3$, the equations look like equations (13–15). And for the last *n*-type layer which is delimited by $d33$ and $d4$ on its borders, the concentration of the minority carrier and the photocurrent density are:

See equations (16) and (17) above.

In the space charge region, we assume that there is no recombination and that every photon absorbed gives rise to an electron-hole pair. The photocurrent density due to the space charge region 1, delimited by $d1$ and $d11$ on its border is:

$$Jscr1 = q\phi\left[\exp\left(-\alpha d1\right) - \exp\left(\alpha d11\right)\right] \quad (18)$$

where α is the absorption coefficient of the silicon and ϕ is the photon flux. The other photocurrent densities are similar and are given by:

$$Jscr2 = q\phi\left[\exp\left(-\alpha d2\right) - \exp\left(\alpha d22\right)\right] \quad (19)$$

$$Jscr3 = q\phi\left[\exp\left(-\alpha d3\right) - \exp\left(\alpha d33\right)\right]. \quad (20)$$

3 Results and discussion

The photocurrent densities in each abscissa of the cell were simulated versus the different layers abscissas under the solar spectrum Air Mass 0 (AM0) [2]. The different equations that expresses the photocurrent densities in both sides of the space charge regions and inside it, say equations (12, 14, 15, 17–20), were introduced into Matlab software with the other physics parameters of the model: the minority carrier diffusion coefficient and the minority carrier lifetime for each layer of the cell. We computed the nine photocurrent densities varying the layers thickness until we reach the maximum value of their sum *JTot*.

The results of simulation are given in Figures 3–5; we can verify that all the boundary conditions (minority carrier concentration) that are defined to solve the differential equations, are respected.

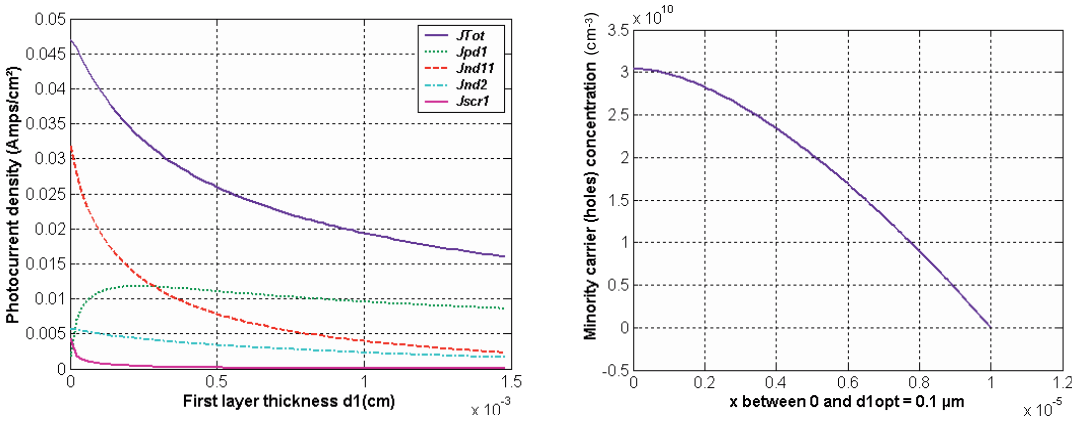

Fig. 3. Optimization of the first layer: the left figure represents the photocurrents versus the thickness of the first layer $d1$, the photocurrent density $JTot$ is the upper curve. The right figure is the minority carriers' density. The optimal abscissa is $d1_{opt} = 0.1$ μm.

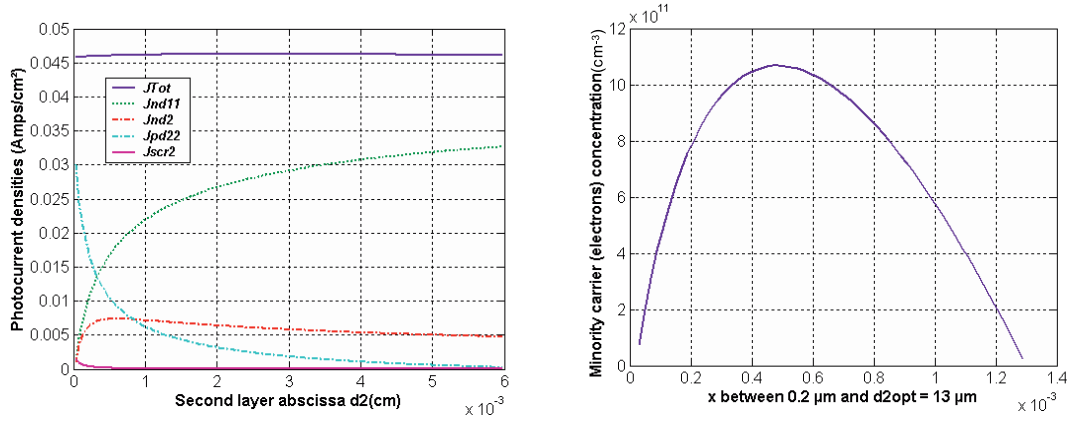

Fig. 4. Optimization of the second layer: the left figure represents the photocurrents versus the thickness of the second layer $d2$, the photocurrent density $JTot$ is the upper curve. The right figure is the minority carriers' density. The optimal abscissa is $d2_{opt} = 13$ μm.

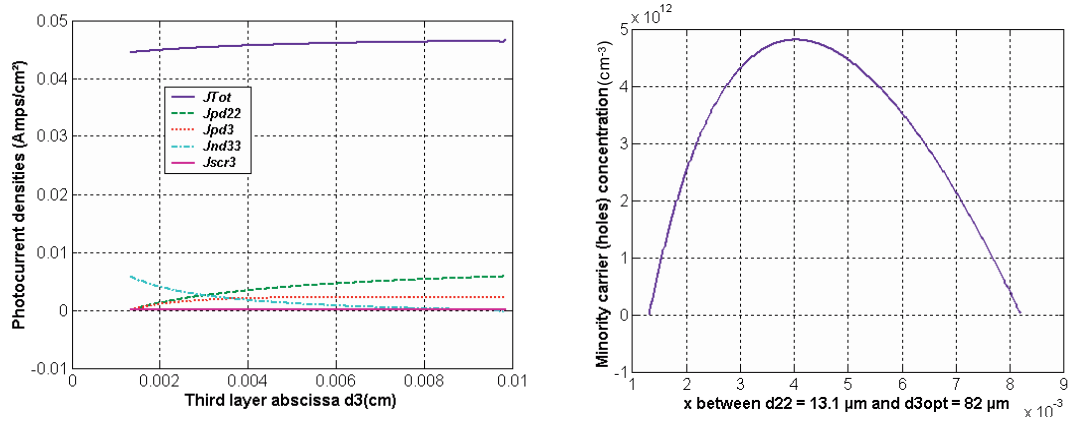

Fig. 5. Optimization of the third layer: the left figure represents the photocurrents versus the thickness of the third layer $d3$, the photocurrent density $JTot$ is the upper curve. The right figure is the minority carriers' density. The optimal abscissa is $d3_{opt} = 82$ μm.

Table 1. Partition of the photocurrent densities.

The total photocurrent density $JTot$	46.28 mA/cm^2	100%
The photocurrent densities due to the three space charge regions	2.43 mA/cm^2	5.25%
The photocurrent densities on both sides of the space charge regions	43.85 mA/cm^2	94.74%

Figure 3 represents the first layer thickness optimization; we simulate the photocurrent densities that are depending on the first layer thickness $d1$, say: $Jpd1$, $Jnd11$, $Jnd2$ and $Jscr1$, $d2$ and $d3$ are maintained constant during this iteration. The maximum photocurrent density $JTot$ is obtained for a first layer thickness $d1$ near zero, we choose $d1$opt equals 0.1 μm that we suppose the minimum thickness giving a homogeneous layer. This thickness gives a total photocurrent density $JTot$ equal to 45.7 mA/cm^2.

The optimization of the second layer thickness defined by the abscissa $d2$, is presented in Figure 4. We simulate the total photocurrent density produced by the multilayer solar cell $JTot$ versus the abscissa $d2$. The photocurrent densities that are depending of the second layer abscissa $d2$, say $Jnd11$, $Jnd2$, $Jpd22$, $Jpd3$, were simulated. The optimal photocurrent is obtained for an abscissa $d2$ equal to 13 μm, and it gives a total photocurrent of 46.01 mA/cm^2.

In Figure 5, we present the simulation of the photocurrent densities that depend of the third layer abscissa $d3$, say $Jpd22$, $Jpd3$, $Jnd33$ and $Jscr3$. We also simulate the total photocurrent density $JTot$ produced by the multilayer silicon solar cell. The optimal third layer abscissa is 82 μm, and it gives a total photocurrent density of 46.28 mA/cm^2.

Finally, the optimal abscissas are: $d1 = 0.1$ μm, $d11 = 0.2$ μm, $d2 = 13$ μm, $d22 = 13.1$ μm, $d3 = 82$ μm and $d33 = 82.1$ μm. The total thickness of the structure was taken equal to 100 μm for mechanical rigidity reasons.
The optimal photocurrent densities are:
$Jpd1 = 5.3$ mA/cm^2,
$Jnd11 = 23.8$ mA/cm^2,
$Jnd2 = 6.9$ mA/cm^2,
$Jpd22 = 5.4$ mA/cm^2,
$Jpd3 = 2.2$ mA/cm^2,
and $Jnd33 = 0.23$ mA/cm^2,
and the photocurrent densities dues to the space charge regions are:
$Jscr1 = 2.4$ mA/cm^2,
$Jscr2 = 0.045$ mA/cm^2
and $Jscr3 = 0.003$ mA/cm^2.
The total photocurrent density produced by the optimized *n-p-n-p* multilayer silicon solar cell is then $JTot$ equal to 46.42 mA/cm^2.

The sum of the photocurrent densities produced by the three space charge regions: $Jscr1$, $Jscr2$ and $Jscr3$ is equal to 2.42 mA/cm^2, which is very low compared to the total photocurrent density $JTot$ (Tab. 1).

4 Summary and conclusion

In this work, we calculated the photocurrent density of a multilayer silicon solar cell for space application; we optimized the thicknesses of the layers that give the maximum photocurrent density under AM0. This represents the first step of a theoretical study of our model. The second step will deal with the open circuit voltage, the series resistance and the fill factor of the same model.

The optimization was achieved using realistic parameters of medium quality material. The equations giving the photocurrent density in each layer of the cell have been developed. We used Matlab software to simulate and optimize the layers thicknesses of the model. Our computation showed that the photocurrent densities produced by the three space charge regions of the cell represent only 5.25% of the total photocurrent density, and that the most important component of the photocurrent density is produced by the collection of the minority carriers, which happens on both sides of the space charge regions, especially in the frontal layers.

Under the optimum conditions, our *n-p-n-p* multilayer cell delivers a photocurrent density of 46.28 mA/cm^2, The optimization of the layers thickness enhances the minority carriers collection, this explains why Brecl et al. [3] model predicts a photocurrent value (28.19 mA/cm^2) much lower than the value predicted by our optimized model (46.28 mA/cm^2).

Note also that, under the same conditions of physical parameters of our model (doping profile, carrier's life time and carriers motilities, etc.), the photocurrent density produced by a simple *n-p* junction silicon solar cell with a junction depth of 0.1 μm and a total thickness of 100 μm is 42.8 mA/cm^2 under AM0 solar spectrum. Thus, the photocurrent density produced by the *n-p-n-p* multilayer silicon solar cell is at least 8.1% higher than the photocurrent density produced by the simple *n-p* junction solar cell, and this represents an important step to achieve very high efficiency solar cell for space applications, which requires more and more efficient solar cells.

References

1. N. Merabtine et al., Quantum Electron. Optoelectron. **7**, 108 (2004)
2. A.S. Bouazzi, M. Abaab, B. Rezig, Sol. Energ. Mat. Sol. C. **46**, 29 (1997)

3. K. Brecl, F. Smole, J. Furlan, Prog. Photovoltaïcs **7**, 449 (1999)
4. A.S. Bouazzi, M. Selmi, Sol. Energ. Mat. Sol. C. (in press)
5. http://www.ioffe.ru/SVA/NSM/Semicond/Si/index.html
6. B. Ba, M. Kane, J. Sarr, Sol. Energ. Mat. Sol. C. **80**, 143 (2003)
7. J.M. Roman, State of the art of III–V solar cell fabrication technologies, devices designs and applications, *Advanced Photovoltaic Cell Design EN548, April 2004*
8. M.J. Keevers, P.P. Altermatt, *16th European Photovoltaic Solar Energy Conference, Glasgow, UK, 1–5 May 2000*
9. M.A. Green, J. Zhao, G.-F. Zheng, *14th European Photovoltaic Solar Energy Conference and Exhibition, Barcelona, 30 June–4 July 1997*
10. J. Zhao, A. Wang, G.-F. Zheng, S.R. Wenham, M.A. Green, *13th European Photovoltaic Solar Energy Conference, October 1995*
11. M.A. Green, S.R. Wenham, Appl. Phys. Lett. **65**, 2907 (1994)